Integration of Single-Stage SPV Generation to Grid using Admittance based LMS Technique

Rahul Kumar Agarwal[1], Ikhlaq Hussain[2] and Bhim Singh[3]

Abstract—In this paper, an integration of single-stage solar photovoltaic (SPV) generation to three-phase AC grid is proposed using admittance based LMS (Least Mean Square) adaptive control approach. The main focus of the system is to supply active power to the grid as well as loads at PCC and also mitigate several power quality issues like current harmonics distortion, reactive power and load unbalancing. A simple LMS based admittance control with P&O (Perturb and Observe) based MPPT (Maximum Power Point Tracking) is used for achieving efficient system. The proposed control is easy to implement and has a fast response. The performance of the system is simulated in MATLAB environment under variable solar irradiance, balanced and unbalanced load (linear and nonlinear) conditions in both PFC and ZVR modes.

Keywords: SPV, P&O, MPPT and Power Quality

I. Introduction

Today grid integration of solar PV (Photovoltaic) systems are emerging technology [1] in the distribution system due to ecofriendly, renewable, battery less, supplying active power to grid as well as loads and mitigates the distribution power quality problems like reactive power load balancing, current harmonics distortions etc. [2-4]. The various configurations of integration of the solar PV systems are single-stage single phase system, double-stage single phase system, single-stage three phase system, double-stage three phase system, single-stage three phase four wire system and double-stage three phase four wire system etc. have been reported in [1-5]. Single-stage topology is demonstrated more operative for applications with higher voltage levels and it has less power losses [6].

The various control algorithms have been reported in to control the VSC (Voltage Source Converter) such as QPLL (Quadrature Phase Locked Loop) [2], EPLL (Enhanced PLL) [3], ANR (Adaptive Noise Reduction) [4]. All these control approaches are used to generate required pulses for VSC in both PFC and ZVR modes. Moreover, in single stage topology different maximum power point tracking (MPPT) approaches have been reported in [7] to generate reference signal for the VSC control algorithm.

In this paper, a single-stage SPV generation is integrated to three-phase distribution grid using a admittance based LMS (Least Mean Square) adaptive control [8] incorporating a perturb and observe (P&O) based MPPT methodology. The proposed control is easy to implement and has very fast response. The performance of the system is simulated in MATLAB environment under variable solar irradiance, balanced and unbalanced loads conditions in both power factor correction (PFC) and zero voltage regulation (ZVR) modes.

II. Control Strategy

Figure 1 shows the proposed single stage SPV system connected to three phase distribution grid. The parameters of the system are given in Appendix. The control architecture of the proposed system is shown in Fig. 2. This control approach uses a single-stage converter topology to achieve two basic functions: MPPT and switching of the VSC. The details of the MPPT control and admittance based LMS adaptive control is given in the section below.

A. MPPT Control

Out of different MPPT methods reported in the literature [7], the hill climbing or P&O approach is used here due to its generic nature and simplicity.

B. Admittance based LMS Adaptive Control Approach

1) Estimation of unit templates

From the sensed PCC voltages (v_{ab} and v_{bc}), the phase voltages are obtained from equation in [9] as,

$$v_a = \frac{2v_{ab} + v_{bc}}{3} \quad ; \quad v_b = \frac{-v_{ab} + v_{bc}}{3} \quad ; \quad v_c = \frac{-v_{ab} - 2v_{bc}}{3} \quad (1)$$

The amplitude of terminal voltage (V_t) is estimated as,

$$V_t = \sqrt{\frac{2}{3}(v_a^2 + v_b^2 + v_c^2)} \quad (2)$$

The unit templates of in-phase and quadrature component are estimated as,

$$u_{pa} = \frac{v_a}{V_t} \quad ; \quad u_{pb} = \frac{v_b}{V_t} \quad ; \quad u_{pc} = \frac{v_c}{V_t} \quad (3)$$

[1]*Member, IEEE, Dept. of Electrical Engineering, IIT Delhi, New Delhi, India*
[2,3]*Fellow, IEEE, Dept. of Electrical Engineering, IIT Delhi, New Delhi, India*
E-mail: [1]rahul.agarwal990@gmail.com, [2]ikhlaqb@gmail.com, [3]bhimsingh7nc@gmail.in
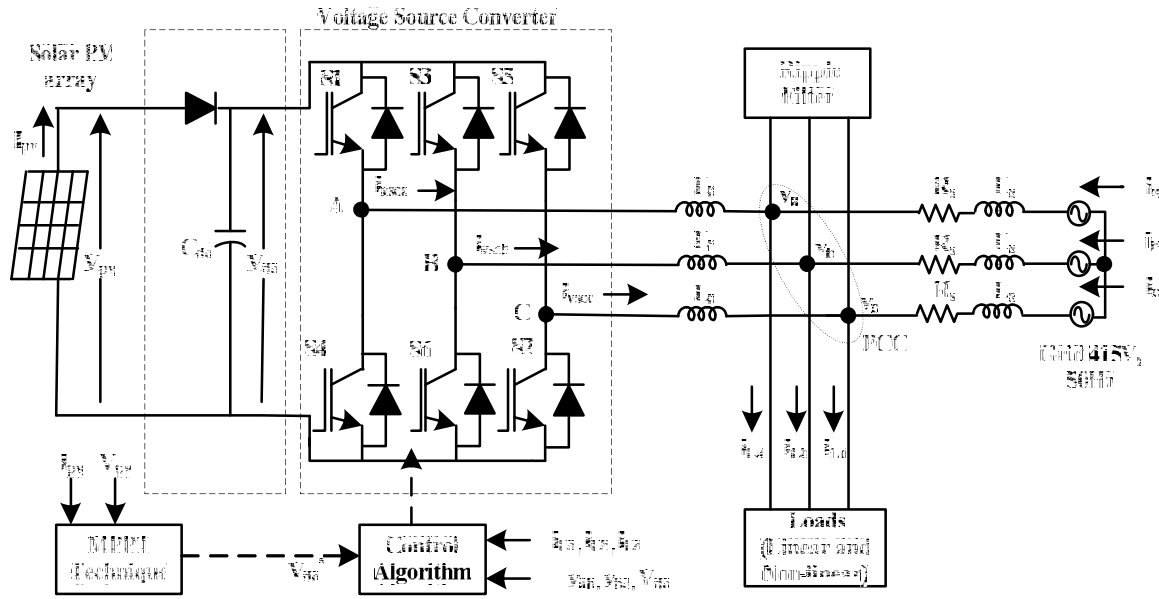
Fig. 1: Proposed system topology.
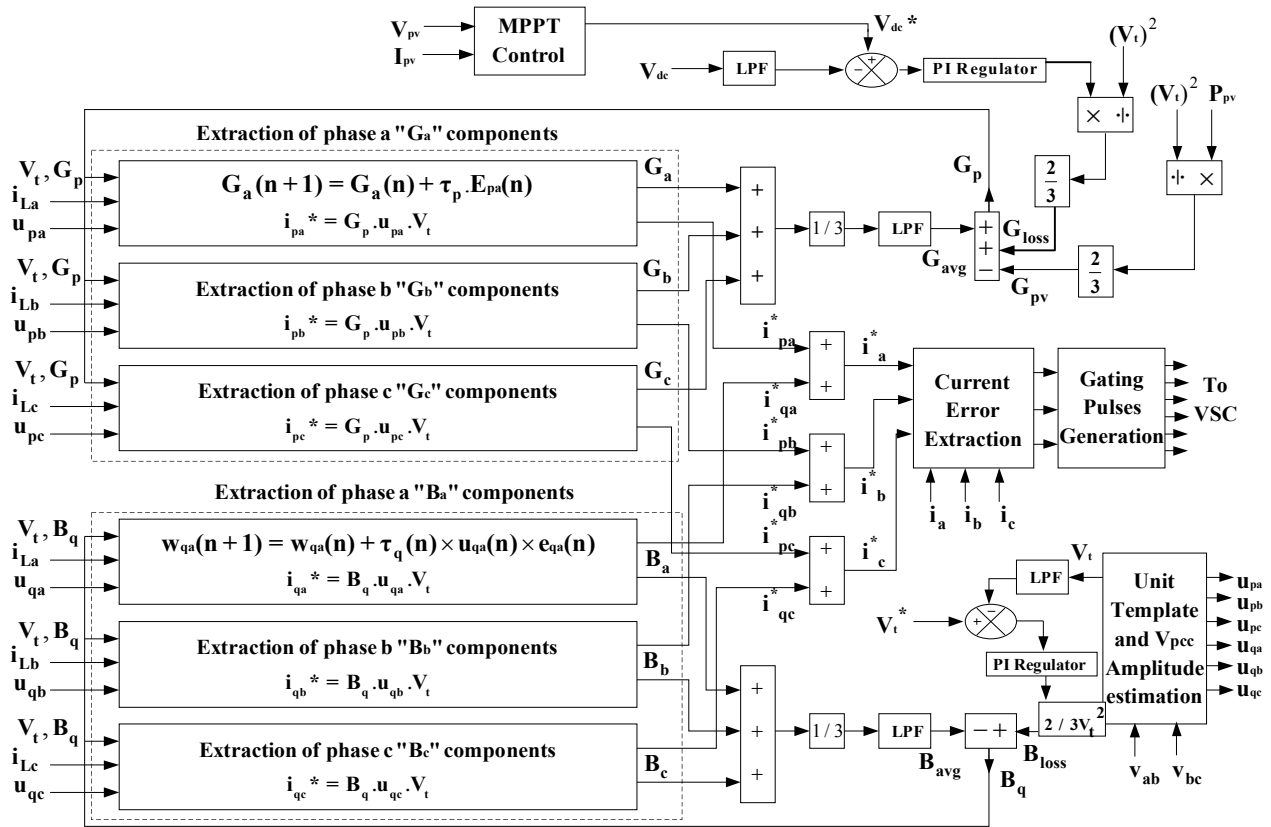
Fig. 2: Control Structure of Admittance based LMS Technique

$$u_{qa} = -\frac{u_{pb}}{\sqrt{3}} + \frac{u_{pc}}{\sqrt{3}} \quad ; \quad u_{qb} = \frac{\sqrt{3}u_{pa}}{2} + \frac{(u_{pb} - u_{pc})}{2\sqrt{3}} \quad ;$$

$$u_{qc} = -\frac{\sqrt{3}u_{pa}}{2} + \frac{(u_{pb} - u_{pc})}{2\sqrt{3}} \tag{4}$$

2) Estimation of admittances of loss components and PV array

After the calculation of terminal voltage V_t, the voltage error $V_{te}(n)$ of the PCC voltage and the reactive loss component (Q_{loss}) are estimated as,

$$V_{te}(n) = V_t^*(n) - V_t(n) \tag{5}$$

$$Q_{loss}(n+1) = Q_{loss}(n) + K_{pt}(V_{te}(n+1) - V_{te}(n)) + K_{it}V_{te}(n+1) \tag{6}$$

Therefore, the susceptance loss component is estimated as,

$$B_{loss}(n) = \frac{2Q_{loss}(n)}{3V_t^2} \tag{7}$$

Where, K_{it} and K_{pt} are integral and proportional gain constants used in PI controller.

Likewise, the DC bus voltage error (V_{de}) and the active loss component (P_{loss}) are calculated as,

$$V_{de}(n) = V_{dc}^*(n) - V_{dc}(n) \tag{8}$$

$$w_{cp}(n+1) = w_{cp}(n) + K_{pd}(V_{de}(n+1) - V_{de}(n)) + K_{id}V_{de}(n+1) \tag{9}$$

Therefore, the susceptance loss component is estimated as,

$$G_{loss}(n) = \frac{2P_{loss}(n)}{3V_t^2} \tag{10}$$

Where, K_{id} and K_{pd} are integral and proportional gain constants used in PI voltage controller.

The total admittance value of the loss components is calculated as,

$$Y_{loss}(n) = G_{loss}(n) + j.B_{loss}(n) \tag{11}$$

The admittance term for the SPV system is estimated as,

$$G_{pv}(n) = \frac{2P_{pv}(n)}{3V_t^2} \tag{12}$$

Where, P_{pv} is extracted SPV power.

3) Extraction of admittances of load current fundamental components

The conductance of fundamental in-phase component of the load current of phase 'a' is evaluated as,

$$G_a(n+1) = G_a(n) + \tau_p.E_{pa}(n) \tag{13}$$

Where, $E_{pa}(n)$ is the error of adaptive component. τ_p is the adaptation constant.

$$E_{pa}(n) = \frac{u_{pa}(n).i_{La}(n).V_t}{v_a^2} - G_a(n) \tag{14}$$

Where, v_a, $i_{La}(n)$ and $u_{pa}(n)$ are the voltage, load current and in-phase unit template at the nth instant of phase 'a'.

Likewise, the conductance of the fundamental in-phase components of other two phases 'b' and 'c' are evaluated as,

$$G_b(n+1) = G_b(n) + \tau_p.E_{pb}(n) \tag{15}$$

$$G_c(n+1) = G_c(n) + \tau_p.E_{pc}(n) \tag{16}$$

The susceptance of fundamental quadrature component of the load current of phase 'a' is evaluated as,

$$B_a(n+1) = B_a(n) + \tau_q.E_{qa}(n) \tag{17}$$

Where, $E_{qa}(r)$ is the error of adaptive component and τ_q is the adaptation constant.

$$E_{qa}(n) = \frac{u_{qa}(n).i_{La}(n).V_t}{v_a^2} - B_a(n) \tag{18}$$

Where, $i_{La}(n)$ and $u_{qa}(n)$ are the load current and quadrature unit template at the nth instant of phase 'a'.

Likewise, the susceptance of the fundamental quadrature components of phases 'b' and 'c' are evaluated as,

$$B_b(n+1) = B_b(n) + \tau_q.E_{qb}(n) \tag{19}$$

$$B_c(n+1) = B_c(n) + \tau_q.E_{qc}(n) \tag{20}$$

4) Generation of reference grid currents

The total conductance component (G_p) of reference grid currents is estimated as,

$$G_p = G_{avg} + G_{loss} - G_{pv} \tag{20}$$

Where, $G_{avg} = (G_a + G_b + G_c)/3 \tag{21}$

Now, the in-phase reference components of grid currents are expressed as,

$$i_{pa}^* = G_p.u_{pa}.V_t \quad ; \quad i_{pb}^* = G_p.u_{pb}.V_t \quad ; \quad i_{pc}^* = G_p.u_{pc}.V_t \tag{22}$$

Similarly, the total susceptance component (B_q) of the reference grid is expressed as,

$$B_q = B_{loss} - B_{avg} \tag{23}$$

Where, $B_{avg} = (B_a + B_b + B_c)/3 \tag{24}$

Now, the reactive reference grid current components are expressed as,

$$i_{qa}^* = B_q.u_{qa}.V_t \quad ; \quad i_{qb}^* = B_q.u_{qb}.V_t \quad ; \quad i_{qc}^* = B_q.u_{qc}.V_t \tag{25}$$

So, the total reference three-phase grid currents are given as,

$$i_a^* = i_{pa}^* + i_{qa}^* \; ; \; i_b^* = i_{pb}^* + i_{qb}^* \; ; \; i_c^* = i_{pc}^* + i_{qc}^* \tag{26}$$

For generation of the gate signals, an indirect current control method is employed with a hysteresis controller as reported in [9].

III. RESULTS AND DISCUSSION

The model of proposed system is validated through simulations carried on a MATLAB/Simulink platform. The solar PV array and other essential components like interfacing inductances, DC link capacitor, ripple filter etc. are designed and modeled as in [9]. The system is subjected to several conditions such as unbalanced and

balanced loads (linear or nonlinear) and varying solar irradiance to verify the system performance. The details of the system parameters is given in Appendix.

A. Performance under Linear Loads

The steady state responses of the system when subjected to linear loads under balanced condition is shown in Fig. 3. The DC link voltage (V_{dc}) is regulated near 700 V and the grid currents (i_{abc}) are maintained sinusoidal. Moreover, the grid absorbs excess power (P_g) from the SPV array and reactive
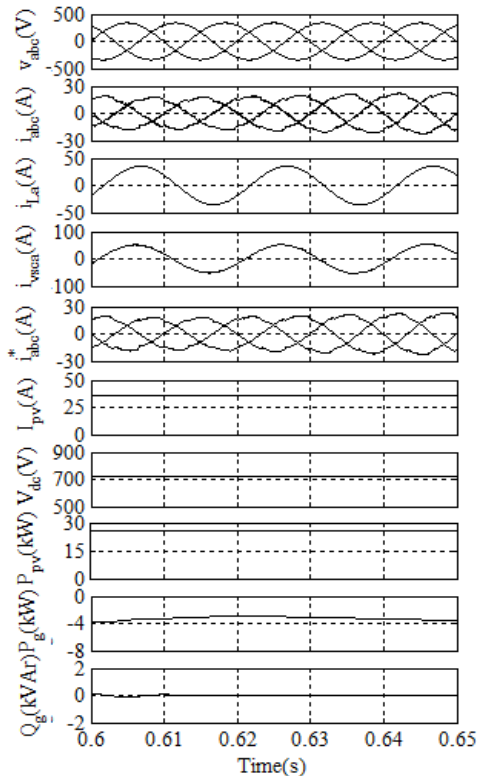
Fig. 3: Steady State Performance under Linear Load

power (Q_g) is maintained near to zero. The system operates at UPF (Unity Power Factor) mode. Table I shows the performance of the system in terms of THD under linear loads. The THD on the grid side is within limits stated by the IEEE-519 standard [9].

B. Performance under Unbalanced Linear Loads

Figures 4 (a-b) show the dynamic performance when subjected to linear unbalanced load. It is observed that when the load of phase 'a' is disconnected at 0.75 s, the grid currents (i_{abc}) are maintained balanced and sinusoidal and these are increased in magnitude as the load draws less power from the SPV array. The DC link voltage (V_{dc}) is nearly constant and system operates at UPF mode. The variation in the internal signals is shown in Fig. 4 (b). The

conductance components (G_{avg} and G_p) are decreased accordingly as the load is disconnected.

C. Performance under Nonlinear Loads

Figure 5 shows the steady state response of the system when subjected to nonlinear loads. Owing to the nonlinearity in the waveform of the load current (i_{La}), the grid currents (i_{abc}) are free from such nonlinearity and harmonics. The DC link voltage (V_{dc}) is retained constant and the system operates at UPF. Table I shows the performance of the system in terms of THD under nonlinear loads. The THD on the grid side is within limits stated by the IEEE-519 standard [9].
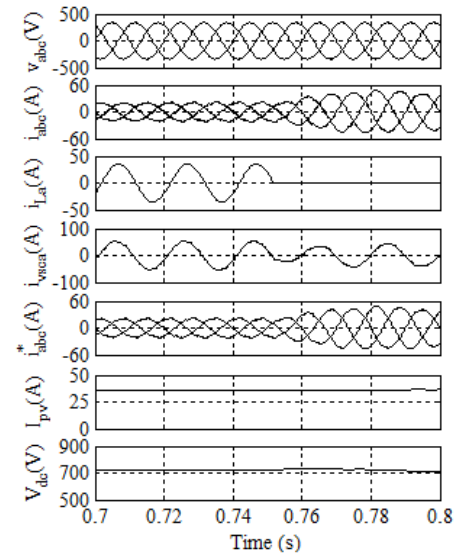
(a)
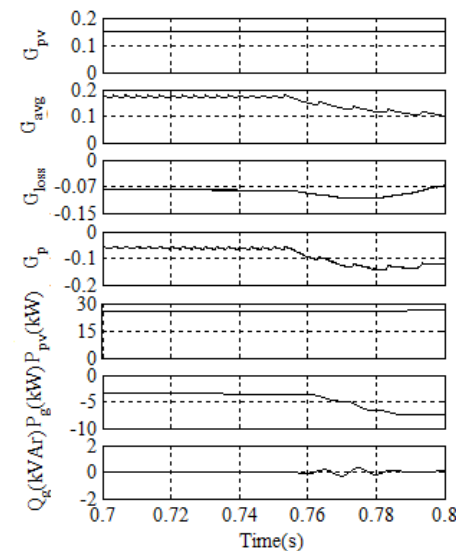
(b)

Fig. 4: (a) Dynamic Performance under Unbalanced Linear Load and (b) Response of Internal Signals
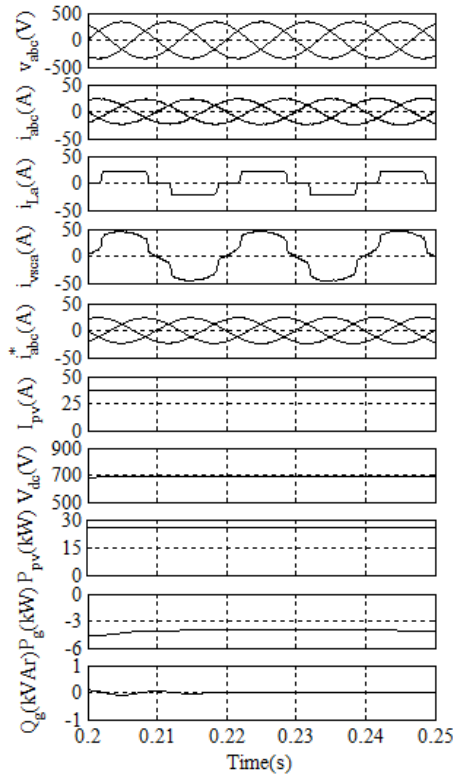
Fig. 5: Steady State Responses under Nonlinear Load

D. Performance under Unbalanced Nonlinear Loads

Figures 6 (a-b) show the dynamic performance of the system subjected to nonlinear unbalanced loads. The load of phase 'a' is disconnected at 0.25 s, and the grid currents (i_{abc}) are maintained balanced and sinusoidal and there are increased accordingly as the load draws less power. The DC link voltage (V_{dc}) is nearly constant and the system operates in UPF mode. The response of internal signals are shown in Fig. 6 (b) and it is observed that the conductance components (G_{avg} and G_p) are decreased and the grid absorbs more power (P_g) from the SPV array.

E. Performance under Variable Solar Insolation

Figure 7 shows the dynamic response of the system when subjected to varying solar intensity. The solar intensity of the PV array is increased from 700 W/m^2 to 1000 W/m^2 at 0.3 s. The SPV array operating point shifts to next maximum power operating point and accordingly grid currents (i_{abc}), VSC currents (i_{vsc}) and PV current (I_{pv}) are increased. The DC link voltage (V_{dc}) is nearly constant, grid currents (i_{abc}) are maintained sinusoidal and the system operates in UPF mode.

(a)

(b)
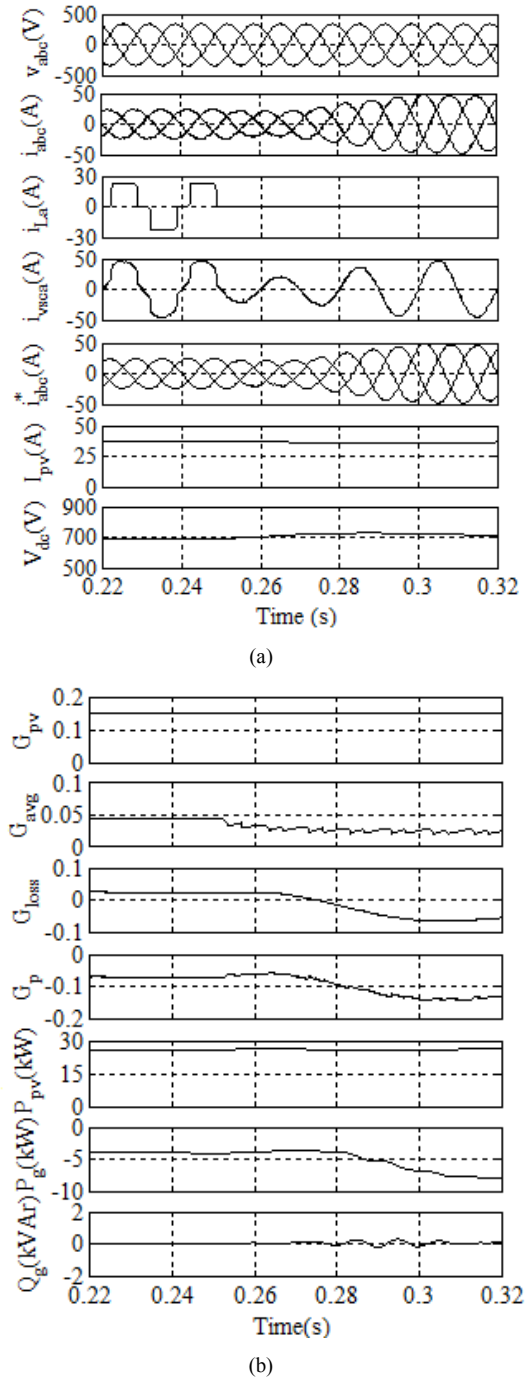
Fig. 6: (a) Dynamic Performance under Unbalanced Nonlinear Load and (b) Response of Internal Signals
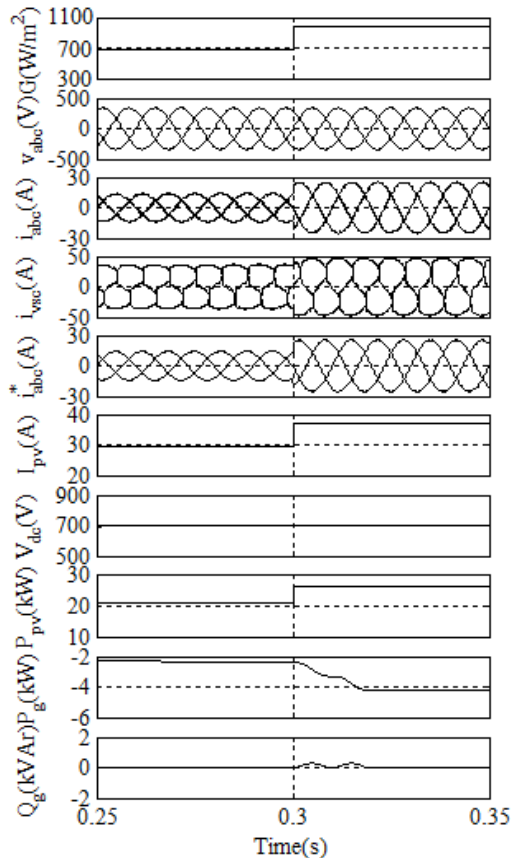
Fig. 7: Dynamic Performance under Variable Solar Insolation

TABLE 1: PERFORMANCE OF THE SYSTEM IN TERMS OF THD

Operation	Parameters	Values of Performances Indices	
		Linear Loads	Nonlinear Loads
UPF	Grid current (A), % THD	20.84 A, 2.38 %	24.93 A, 1.26 %
	Load current (A), % THD	35.42 A, 3.21 %	24.55 A, 27.6 %
	VSC current (A), % THD	53.68 A, 1.71 %	49.38 A, 13.7 %

IV. CONCLUSION

The proposed single-stage solar photovoltaic (SPV) generation has been integrated to three-phase AC grid using admittance based LMS (Least Mean Square) adaptive control technique. The system supplies active power to grid as well as connected loads and also mitigates several power quality issues like current harmonics distortion, reactive power, load unbalancing etc. A simple LMS based admittance control with P&O based MPPT has been found easy to implement and has a fast response. The performance of the system has been simulated in MATLAB environment under variable solar

irradiance, balanced and unbalanced loads conditions in both PFC and ZVR modes.

V. APPENDIX

A. System Parameters

SPV array voltage, V_{MPP} = 700 V; array current, I_{MPP} = 38 A; array power, P_{MPP} = 26 kW; DC Bus Voltage, V_{dc} = 700 V; DC bus capacitor, C_{dc} = 6000 µF; interfacing inductor, L_f = 2.5 mH; sampling time, T_s = 1 µs; grid voltage, V_{LL} = 415 V (rms); ripple filter, R_f = 5 Ω and C_f = 10 µF, DC PI controller, K_{pd} = 1.5 and K_{id} = 1; Adaptation constant, τ = 1.25; linear load with P = 15kW and Q = 10 kVAr; nonlinear load = 3-phase diode bridge feeding load R = 25 Ω and L = 150 mH.

REFERENCES

[1] S. Kouro, J. I. Leon, D. Vinnikov, and L. G. Franquelo, "Grid-connected photovoltaic systems: an overview of recent research and emerging PV converter technology," *IEEE Ind. Electron. Mag.*, vol. 9, no. 1, pp. 47-61, March 2015.

[2] B. Singh, S. Dwivedi, I. Hussain and A. K. Verma, "Grid integration of solar PV power generating system using QPLL based control algorithm," in *Proc. 6th IEEE Power India Int. Conf.*, 5-7 Dec. 2014, pp. 1-6.

[3] S. Kumar, A. K. Verma, I. Hussain and B. Singh, "Performance of grid interfaced solar PV system under variable solar intensity," in Proc. *IEEE 6th India Int. Conf. on Power Electronics*, 8-10 Dec. 2014, pp. 1-6.

[4] B. Singh, S. Goel, A. Singhal, A. Garg and C. Jain, "Power quality enhancement of grid integrated solar PV system based on adaptive noise reduction control," in *Proc. IEEE Power & Energy Society General Meeting*, 26-30 July 2015, pp.1-5.

[5] A. K. Barnes, J. C. Balda and C. M. Stewart, "Selection of converter topologies for distributed energy resources," in *Proc. IEEE 27th Ann. App. Pow. Electron. Conf. Exposi.*, 5-9 February 2012, pp. 1418-1423.

[6] Tsai-Fu Wu, Chih-Hao Chang, Li-Chiun Lin and Chia-Ling Kuo, "Power loss comparison of single-and two-stage grid-connected photovoltaic systems," *IEEE Trans. on Energy Conv.*, vol. 26, no. 2, pp. 707-715, June 2011.

[7] M. A. G. de Brito, L. Galotto, L. P. Sampaio, G. A. Melo and C.A.Canesin, "Evaluation of the main MPPT techniques for photovoltaic applications," *IEEE Trans. on Ind. Electron.*, vol. 60, no.3, pp.1156-1167, March 2013.

[8] B. Widrow, J. M. McCool, M. Larimore and C. R. Johnson, "Stationary and non-stationary learning characteristics of the LMS adaptive filter," *Proc. of IEEE*, vol.64, no.8, pp. 1151-1162, Aug. 1976.

[9] Bhim Singh, Ambrish Chandra and Kamal Al-Haddad, *Power quality: problems and mitigation techniques*, John Wiley & Sons Ltd., U.K, 2015.